Proceedings of the Combustion Institute, Volume 29, 2002/pp. 1461–1469

OUTWARD PROPAGATION, BURNING VELOCITIES, AND CHEMICAL EFFECTS OF METHANE FLAMES UP TO 60 ATM

G. ROZENCHAN,[1] D. L. ZHU,[1] C. K. LAW[1] AND S. D. TSE[2]
[1]*Department of Mechanical and Aerospace Engineering*
Princeton University
Princeton, NJ 08544, USA
[2]*Department of Mechanical and Aerospace Engineering*
Rutgers, The State University of New Jersey
Piscataway, NJ 08854, USA

Using a specially designed high- and constant-pressure combustion chamber, the propagation and morphology of spark-ignited expanding spherical methane flames were imaged using schlieren cinematography and a high-speed digital camera. Stretch-free laminar burning velocities were subsequently determined for methane/air flames up to 20 atm and methane/oxygen/helium flames up to 60 atm. Computational simulation using GRI-MECH 3.0 showed satisfactory agreement with the experimental data up to 20 atm, and moderate deviation for pressures above 40 atm. Markstein lengths, global activation energies, and overall reaction orders were also determined as functions of pressure, with the latter two parameters exhibiting non-monotonic behavior caused by the changeover from H-O_2 to HO_2 chemistry similar to that of the explosion limits of homogeneous hydrogen/oxygen mixtures.

Introduction

Recent studies on combustion chemistry have identified the need for high-pressure kinetics for application in internal combustion engines, which typically operate under elevated pressures on the order of 10–100 atm. Such a need can best be appreciated by considering the potential limitations of the widely used GRI-MECH developed for methane oxidation [1]. Specifically, the development involves optimizing the subject mechanism against a set of known performance targets covering combustion phenomena ranging from low- to high-temperature chemistries [2,3]. These would include, for example, ignition delays in shock tubes, ignition and extinction limits in perfectly stirred reactors, laminar burning velocities, and ignition, extinction, and structure of premixed and non-premixed flames. Furthermore, in order to be as extensive as possible in the ranges of thermodynamic coverage, the mixture concentration should vary from very lean to very rich, while the system pressure should also vary from moderately subatmospheric to sufficiently superatmospheric. Regarding the last point, it is then particularly noteworthy that optimization of the GRI-MECH has utilized only one experimental datum for the high-pressure laminar burning velocities, at 20 atm, while its determination also does not appear to carry the degree of accuracy [4] usually required for a study of the present nature. All the remaining targets lie below 5 atm. Because of the inherently nonlinear nature of chemical reactions, this inadequacy could limit the versatility of the mechanism to simulate high-pressure combustion processes with confidence.

In view of the above considerations, the first objective of the present study is to provide reliable laminar burning velocity data for methane at elevated pressures. To meet this goal, we note that laminar burning velocities of methane/oxidizer mixtures at elevated pressures and of high degree of fidelity have been recently reported by several groups. Specifically, Hassan et al. [5] and Gu et al. [6] measured the speeds of outwardly propagating flames in a windowed bomb up to 4 and 10 atm, respectively, and determined the associated laminar burning velocities through systematic subtraction of stretch effects. Steady-state methods, such as those using the counterflow [7,8], modified counterflow [9], and flat flame burner [10], are well established to be quite accurate in measuring the laminar burning velocity with corrections for stretch and heat loss. Their operational range, however, is limited to a few atmospheres due to flame stability problems. Eberius and Kick [11] developed a Bunsen burner in which rich methane/air flames could be stabilized up to 100 atm, but did not correct the data for stretch effects.

In response to the need for high-pressure burning velocity data, a windowed, dual-chambered bomb was developed for the study of high-pressure combustion phenomena up to 60 atm [12]. This apparatus was employed to determine the laminar burning velocities of hydrogen mixtures up to 20 atm

[12], with the upper range being limited by the profuse development of hydrodynamic and diffusional-thermal cells over the flame surface. In the present investigation, we used this apparatus to determine the much-needed high-pressure laminar burning velocity data for methane mixtures. Because of the reduced propensity of methane flames to form cells as compared to hydrogen flames, we shall show in due course that laminar burning velocities up to 60 atm have been successfully determined.

Having determined the laminar burning velocities, our second objective is to compare them with the computed ones using GRI-MECH. Through such a comparison, the performance of the mechanism in terms of high-pressure application can be assessed.

The third objective is to study the pressure dependence of two additional global flame parameters of interest, namely the Markstein length, which quantifies the sensitivity of the flame to stretch, and the overall reaction order, which yields the dependence of the burning rate on pressure. The influence of chemistry on these global parameters, especially over the present extensive range of high-pressure variation, will be identified.

In the following, we shall first discuss the experimental and computational methods and then present the results on flame morphology, laminar burning velocities, Markstein lengths, and overall reaction orders.

Experimental and Computational Methods

The design and operation of the double-chambered, near-constant-pressure apparatus utilized in the present experiment is described in detail in Refs. [12] and [13]. This design allows an order-of-magnitude increase in the attainable experimental pressure over single chamber designs [5,6] by filling the outer chamber with an inert mixture to absorb the pressure buildup during flame propagation and to terminate the propagation before the pressure buildup becomes substantial. Grade 4.0 methane and gas chromatograph-calibrated oxidizer mixtures were used in the experiments. Fuel-oxidizer mixtures were periodically sampled for GC-concentration verification, and the results presented were averaged over three to four experiments for each point. The initial gas temperature was kept at 298 K. The ignition energy was kept to a minimum so as to minimize initial flame acceleration. Data reduction was performed only for flame radii (r) between 0.5 and 2 cm so as to avoid possible effects caused by spark disturbance and wall interference.

For the outwardly propagating flame, the burned gas is motionless. Thus, for weak stretch, the local burned flame speed $s_b = \dot{r} = dr/dt$ can be linearly related to the instantaneous stretch rate $\kappa = 2\dot{r}/r$ via $s_b = s_b^0 - L_b\kappa$ [14–16], where s_b^0 is the unstretched downstream laminar burning velocity ($\rho_b s_b^0 = \rho_u s_u^0 = f^0$), L_b the burned Markstein length, ρ the density, and f^0 the laminar burning flux. Integrating this relation with respect to time yields

$$r + 2L_b \ln(r) = s_b^0 t + \text{constant} \qquad (1)$$

Thus, s_b^0 and L_b can be obtained by linear regression through the measurement of radius evolution with time. Knowing s_b^0, the (unburned) laminar burning velocity s_u^0 can be readily evaluated from the density ratio across the flame.

Numerical simulation of adiabatic, one-dimensional, planar flames was carried out with the PREMIX code [17] using the GRI-MECH 3.0 mechanism [1] for all flames studied and also the GRI-MECH 1.2 [18] for helium-diluted flames; the need to use helium will be discussed shortly. The GRI-MECH 2.11 version was not used because it is essentially identical to the 1.2 version with respect to the carbon-hydrogen-oxygen chemistry [19].

For both mechanisms, third-body efficiencies of argon were used for helium, and reactions involving nitrogen compounds were removed in the simulation of He-diluted flames. Radiative heat loss through CO_2 and H_2O were found to have little influence on the computed laminar flame speeds and hence were neglected. Soot radiation was also not included in the calculation because soot was not detected in the experiments.

Results and Discussion

Flame Morphology

Figure 1 shows that the atmospheric CH_4/air flame has a smooth surface throughout propagation. Wrinkling, however, emerges as pressure increases. At 10 atm, Fig. 1 shows that these wrinkles are triggered by the spark or electrode perturbations and remain similar in morphology as the flame expands. The absence of cell cracking to smaller scales and hence flame acceleration due to self-similar propagation [20–22] suggest that the linear relationship between flame speed and stretch still holds, and therefore the laminar burning velocities can be meaningfully extracted at these pressures.

Above 20 atm, cell cracking is observed. Two strategies were implemented in order to allow smooth flame propagation at higher pressures: higher inert dilution in the oxidizer and the use of helium as inert. The former weakens the flame, increasing the flame thickness δ and decreasing the density ratio across it, thereby delaying the onset of hydrodynamic instability [23,24]. The latter, due to helium's higher diffusivity with respect to nitrogen, simultaneously increases δ and the mixture Lewis number

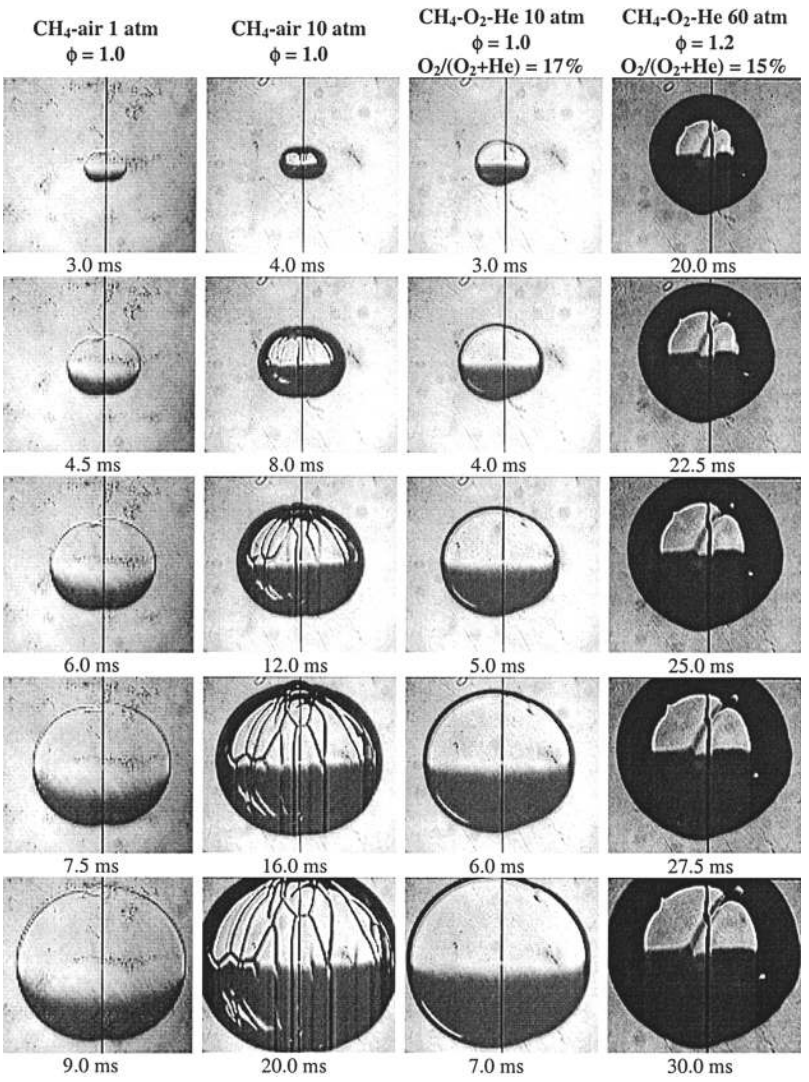

FIG. 1. Schlieren photographs (horizontal knife-edge) of CH_4/O_2/inert flames under stoichiometric and rich conditions. Scale: frame width is 41.4 mm.

Le, suppressing thermal-diffusive instability [23,25]. Higher N_2 dilution proved ineffective because of the slower flame speed and consequently distortion of the flame shape due to buoyancy. With high levels of He dilution, smooth flames with only a few large wrinkles were observed up to 60 atm, as shown in Fig. 1.

Laminar Burning Velocities

The extracted laminar burning velocities of CH_4/air at 1 atm from the measured stretch-affected flame propagation speeds are shown in Fig. 2a, along with other recent experimental results in the literature [5,6,8–10]. The overall agreement among the experimental data is quite satisfactory, providing a benchmark for accuracy and reliability of the present apparatus and experimental methodology. Fig. 3 depicts the laminar burning velocities at 2 and 5 atm, along with other experimental results [5,6,26]. Good agreement is again observed.

Figures 4 and 5 show the burning velocities of CH_4/air and CH_4/O_2/He mixtures at 10, 20, 40, and 60 atm, together with the data of Gu et al. [6] for 10 atm CH_4/air mixtures. We first note that the data of Gu et al. agree well with the present data. Since there are basically no literature data available either at higher pressures or for the special He-diluted composition, comparison can only be conducted

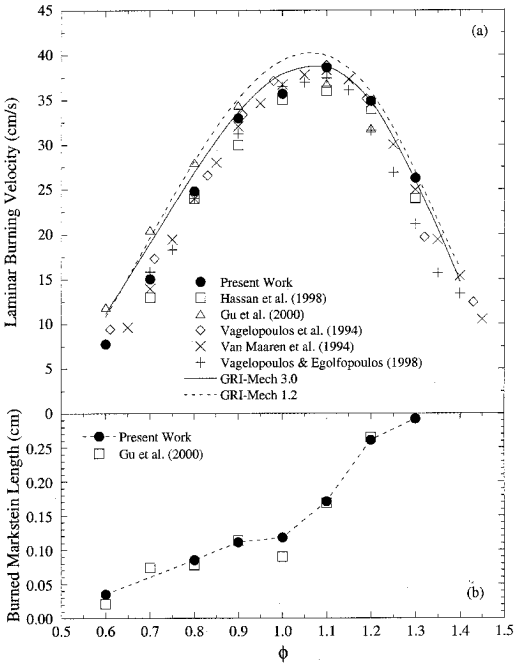

FIG. 2. (a) Laminar burning velocities and (b) Markstein lengths of CH_4/air mixtures at 1 atm as a function of equivalence ratio. Measurements are from Hassan et al. [5], Gu et al. [6], Vagelopoulos et al. [8], Van Maaren et al. [10], and Vagelopoulos and Egolfopoulos [9]. Symbols represent experimental data; lines represent calculation.

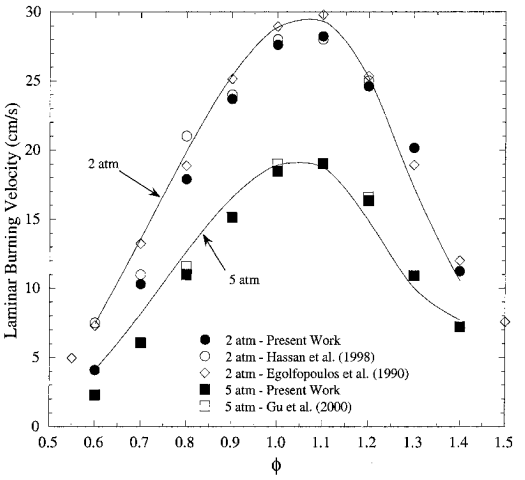

FIG. 3. Laminar burning velocities of CH_4/air mixtures at 2 and 5 atm as a function of equivalence ratio. Measurements are from Hassan et al. [5], Egolfopoulos et al. [26], and Gu et al. [6]. Symbols represent experimental data; lines represent calculation with GRI-MECH 3.0 [1].

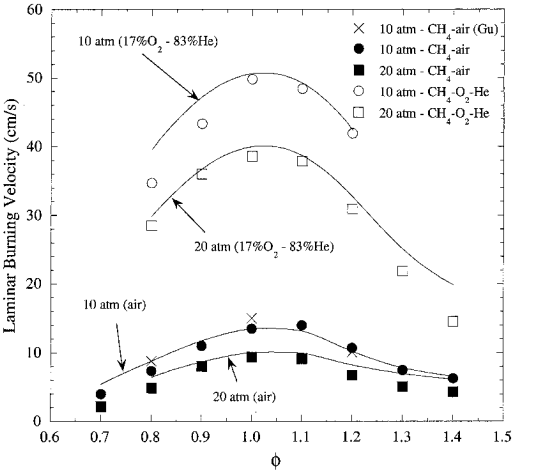

FIG. 4. Laminar burning velocities of CH_4/air and CH_4/O_2/He [$O_2/(O_2 + He) = 17\%$] mixtures at 10 and 20 atm as a function of equivalence ratio. Measurements are from Gu et al. [6]. Symbols represent experimental data; lines represent calculation with GRI-MECH 3.0 [1].

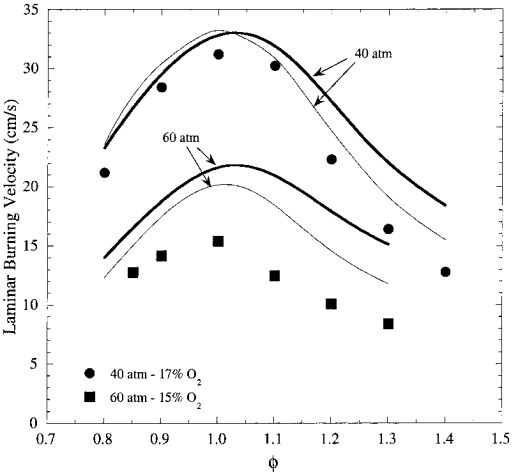

FIG. 5. Laminar burning velocities of CH_4/O_2/He mixtures at 40 and 60 atm as a function of equivalence ratio and with different O_2 concentrations in the O_2/He oxidizer mixture. Symbols represent experimental data; thick lines represent calculation with GRI-MECH 3.0 [1], while thin lines represent calculation with GRI-MECH 1.2 [18].

with the computed results. It is seen that while the comparison is mostly satisfactory for the 10–20 atm flames, the agreement is not as good as those at lower pressures. The extent of discrepancy progressively increases, both in magnitude and the range of the equivalence ratio, as the pressure is increased to 40 and 60 atm. While various postulates can be made regarding the discrepancy, such as the efficiency of

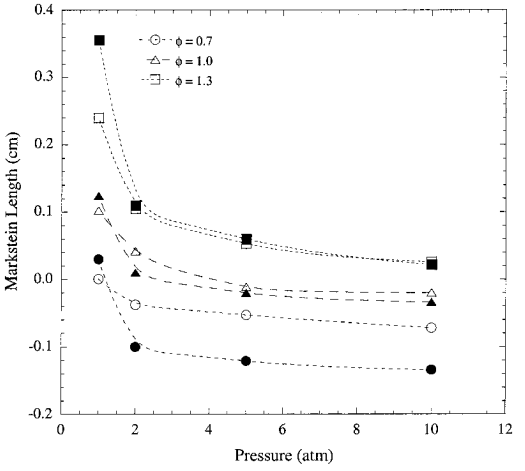

FIG. 6. Burned (open symbols) and unburned (closed symbols, $\times 10$) Markstein lengths of CH_4/air flames as a function of pressure for fixed equivalence ratios.

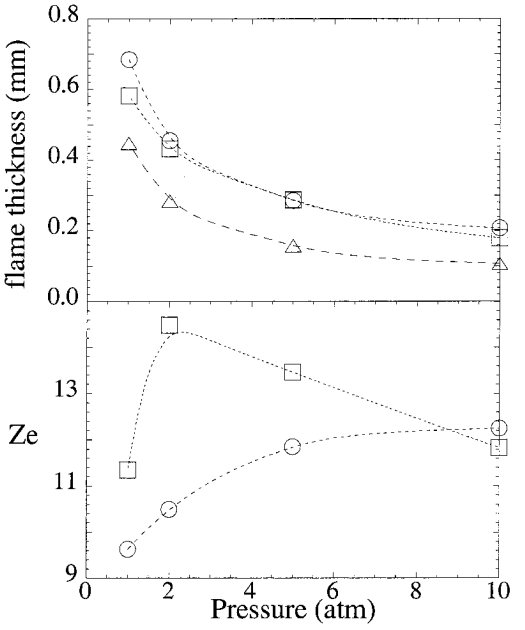

FIG. 7. Calculated flame thicknesses (top) and Zeldovich numbers (bottom) for the data of Fig. 6.

He as a third body in termination reactions and the emphasis on NO_x chemistry [1] in version 3.0, we shall refrain from being specific because of the large departure of the present pressure range from those used in the mechanism development and consequently the significant uncertainty involved in the "extrapolation." These data are simply presented for further studies by our colleagues.

Markstein Lengths

The Markstein length characterizes the flame response to stretch [25,27,28] and was determined along with the laminar burning velocity according to equation 1. Fig. 2b shows that for CH_4/air at 1 atm, the burned Markstein lengths agree very well with the results of Gu et al. [6]. Fig. 6 plots the variation of the Markstein length with pressure, for a lean ($\phi = 0.7$), a rich ($\phi = 1.3$), and the stoichiometric flames, showing that L_b decreases with pressure for a given equivalence ratio. To interpret this behavior, we consider the expression for the Markstein length [25,28], $L_b \sim Ze(Le - 1)\delta$, where $Ze = E_a(T_b^0 - T_u)/R(T_b^0)^2$ is the Zeldovich number, E_a the activation energy, T_b^0 the adiabatic flame temperature, T_u the freestream temperature, and R the universal gas constant. The expression for L_b shows the three main factors that determine the response of the burning velocity to stretch variations, namely Le, δ, and Ze. Non-equidiffusion, represented by $Le \neq 1$, determines the sign of L_b and hence the trend of the flame response to stretch. For the present positively stretched, outwardly propagating flame, $L_b > 0$ (<0) corresponds to $Le > 1$ (<1). The flame thickness δ controls the transit time of the reactants in crossing the flame. Fig. 7 (top) plots the calculated values of δ from the temperature profile of the numerical solution according to the gradient definition, $\delta = (T_b^0 - T_u)/(dT/dx)_{max}$ [27,28] and shows that δ continuously decreases with pressure. This is to be expected because the laminar burning flux continuously increases with pressure. The Zeldovich number measures the sensitivity of the reaction rate to the flame temperature and is plotted in Fig. 7 (bottom), with E_a determined from the variation of the laminar burning flux with the adiabatic flame temperature [27,28]. It is seen that Ze increases with pressure for the lean mixture, reflecting the progressive importance of the three-body termination reactions. For rich mixtures, however, Ze first increases and then decreases. This indicates the influence of some additional competing chemistry, which turns out to be that involving the branching reactions of HO_2 and H_2O_2 radicals, as will be discussed together with the reaction orders in Figs. 8 and 9. We also note that E_a, and hence Ze, were not determined for the stoichiometric mixture because of the significant inaccuracy associated with extracting E_a around the maximum laminar burning flux. However, regardless of the behavior of Ze, the trend for the variation of L_u should be dominated by that of δ because the extent of variation of Ze within the range of pressure investigated is much smaller than that of δ.

Based on the above considerations, and recognizing that Le for lean and rich CH_4/air mixtures is respectively smaller and greater than unity, it is then reasonable that L_b is positive and decreases with

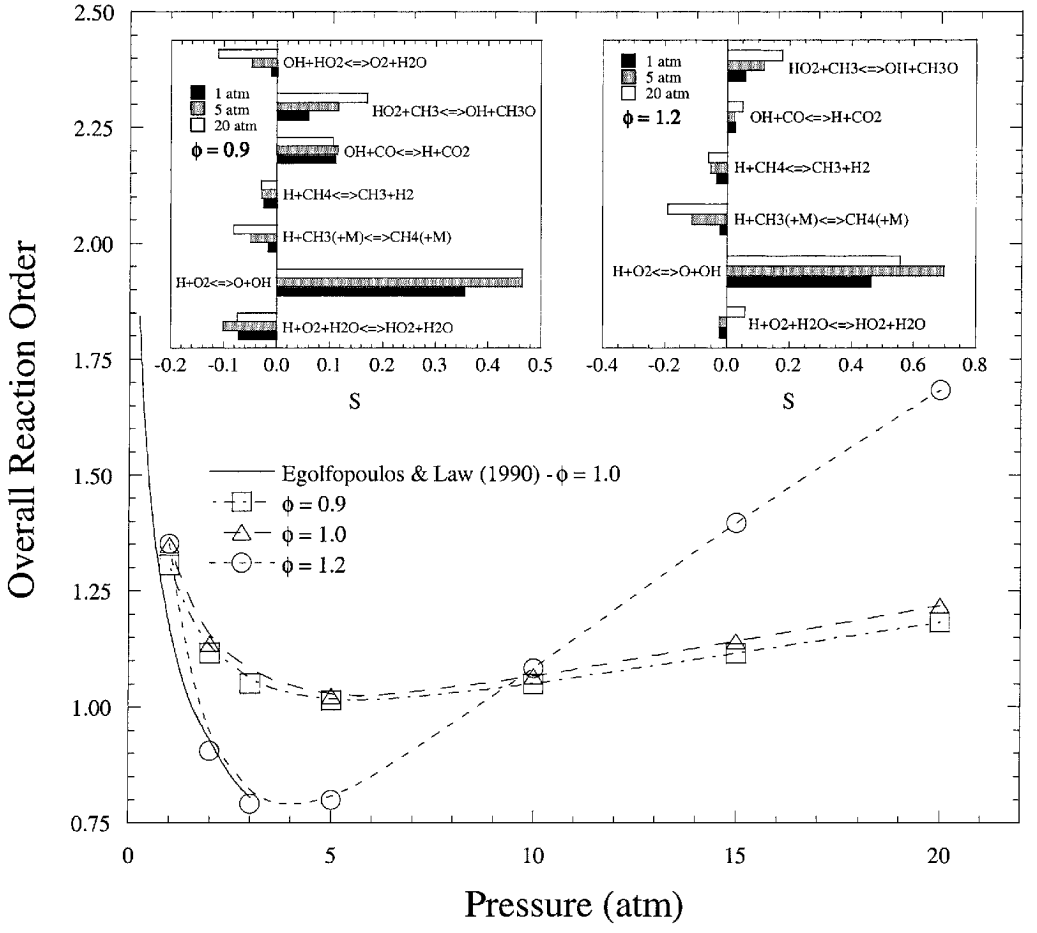

FIG. 8. Overall reaction orders of CH_4/air flames as a function of pressure for fixed equivalence ratios. Results of Egolfopoulos and Law [29] are plotted for comparison. The insets show the normalized sensitivity on mass burning rate (S) for the most important elementary reactions at $\phi = 0.9$ and 1.2.

pressure for the rich mixture and is negative for the lean mixture. The result that the magnitude of the L_b for the lean mixture actually slightly increases with pressure, as previously observed by Hassan et al. [5], cannot be readily explained. Since the flame response is expected to be very sensitive to deviations of *Le* from unity for such near diffusively neutral situations, the flame response can also be affected by other non-equidiffusive factors beyond the single *Le* consideration.

Figure 6 also plots the unburned Markstein lengths (L_u). The definition of L_u follows from the behavior of the burning velocity with respect to the unburned gas, according to Ref. [26] $s_u = s_u^0 - L_u\kappa$. Using continuity across the flame and allowing for mass accumulation within the finite flame thickness, it can be shown [13,27] that $L_u = \sigma L_b - (\alpha - \sigma)\delta$, where $\sigma = \rho_b/\rho_u$ is the density ratio across the flame and $\alpha = \int_0^1 (\rho/\rho_u) d(x/\delta)$ is the factor accounting for mass accumulation within the flame, which can be calculated based on the density profile obtained from the numerical solution of the unstretched flame. It is seen that L_u basically behaves similarly as L_b.

Overall Reaction Orders

Knowing the variation of the laminar burning velocity (s_u^0) with pressure (p) and from the relation $s_u^0 \sim w^{1/2}/\rho_u \sim p^{(n/2)-1}$, the overall reaction orders (n) can be computed [29] from

$$n = 2 + 2\,\frac{\partial \ln(s_u^0)}{\partial \ln(p)} \qquad (2)$$

where ρ_u is the unburned gas density and w the reaction rate. Egolfopoulos and Law [29] obtained values of n for CH_4/air mixtures up to 3 atm, finding

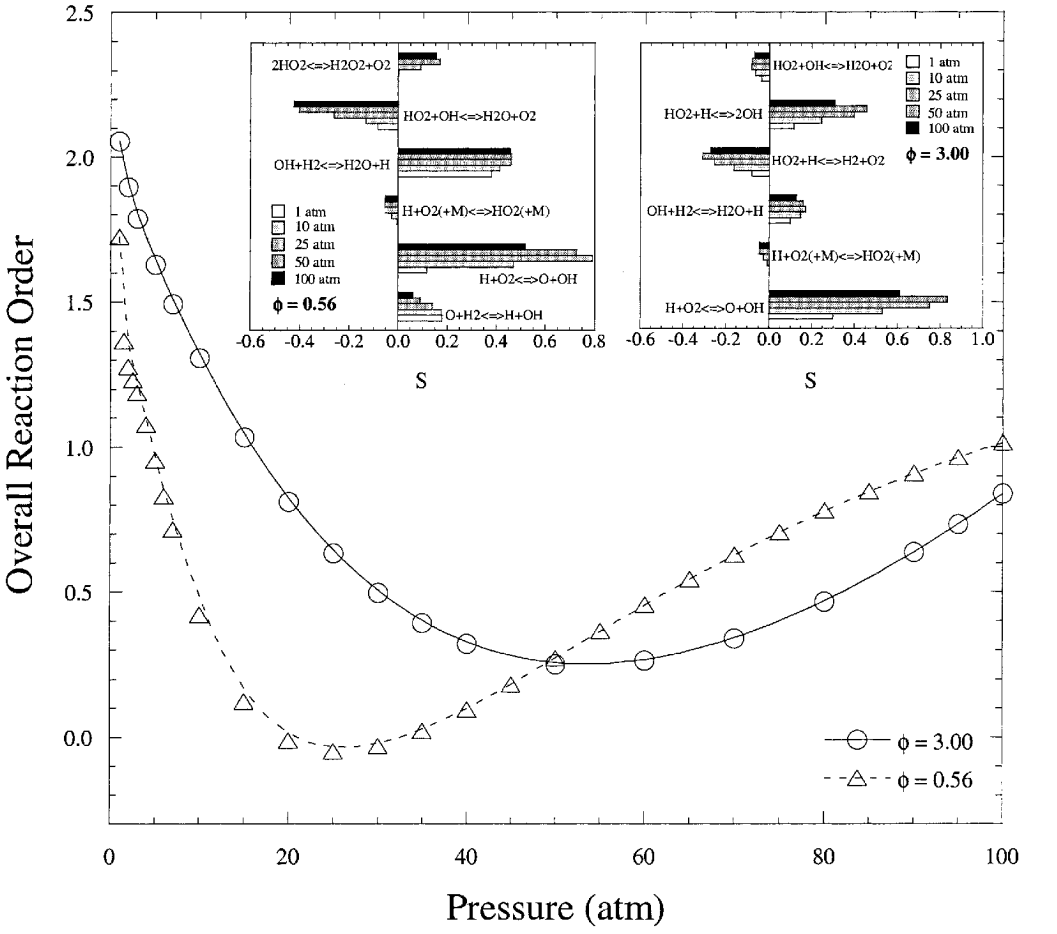

FIG. 9. Overall reaction orders for lean and rich H_2/air flames with $T_b = 1760$ K as a function of pressure. The insets show the normalized sensitivity on mass burning rate (S) for the most important elementary reactions.

that n decreases with pressure for a given ϕ due to the progressive importance of termination reactions over branching reactions. In the present study, the range of pressures was extended by almost an order of magnitude, and it was found that, after reaching a minimum, n increases again with increasing pressure. The increase is particularly prominent for the $\phi = 1.2$ case, as shown in Fig. 8 for several ϕ and those of Ref. [29] for $\phi = 1.0$. It is seen that this non-monotonic behavior was not previously detected [29] due to the limited pressure range studied. The fact that the present results on $\phi = 1.0$ quantitatively deviate from those of Ref. [29] is due to the different mechanisms used and the sensitivity in the extraction of n. Furthermore, the different experimental methods used in the determination of the laminar burning velocities could have also contributed to the difference.

This non-monotonic behavior of n with pressure suggests an analogy with the three explosion limits of hydrogen/oxygen mixtures. The second limit, which corresponds to the increasing importance of termination over branching reactions, leads to the initial decrease of n with pressure, as identified in Ref. [29]. The third limit corresponds to the regime in which n increases with pressure and would be due to the new branching pathways at high pressures [30].

To identify the cause for this increase, sensitivity analysis [$S_i = (k_i/f^0)\partial f^0/\partial k_i$, where k_i is the reaction rate for the ith elementary reaction] was carried out [17], and the influence of the main branching and termination reactions on the mass burning rate was evaluated. It was found that the increasing sensitivity of the termination reactions $H + O_2 + M \rightarrow HO_2 + M$ and $H + CH_3(+M) \rightarrow CH_4(+M)$ as compared to that of the main branching reaction, $H + O_2 \rightarrow O + OH$, causes the initial decrease in n, which reaches a minimum between 3 and 5 atm. Above 5 atm, the new branching reaction $HO_2 +$

$CH_3 \rightarrow OH + CH_3O$ becomes very active and contributes to the subsequent increase in n again by supplying the flame with the OH radical, which is further used by the chain carrying step $OH + CO \rightarrow H + CO_2$. This new branching pathway is also responsible for the observed non-monotonic behavior of E_a and hence Ze shown in Fig. 7, as noted earlier.

The finding of the behavior of n with pressure for methane mixtures prompted the investigation of whether the same phenomenon also applies to hydrogen flames. Since hydrogen flames are highly wrinkled above a few atmospheres [12,13], computations were performed with one lean ($\phi = 0.56$) and one rich ($\phi = 3.00$) H_2/air mixture up to 100 atm, both having the same adiabatic flame temperature (1760 K). The overall reaction orders extracted from the numerical results are presented in Fig. 9, which shows the same non-monotonic behavior of n with pressure, but now the minimum n takes place at much higher pressures. Sensitivity analysis showed that the initial decrease of n with pressure is due to the competition between the branching reaction $H + O_2 \rightarrow O + OH$ and the termination reactions $H + O_2 + M \rightarrow HO_2 + M$, $HO_2 + OH \rightarrow H_2O + O_2$ (for lean flames), and $HO_2 + H \rightarrow H_2 + O_2$ (for rich flames). As pressure further increases, HO_2 reactions generate new radicals [31,32] through $2HO_2 \rightarrow H_2O_2 + O_2$, $H_2O_2 + M \rightarrow 2OH + M$, and $HO_2 + H \rightarrow 2OH$. This mechanism for the recovery of n with pressure is completely analogous to that of the explosion limits for H_2/O_2 mixtures.

Concluding Remarks

In the present investigation, we have experimentally determined stretch-free laminar burning velocities of methane/air flames up to 20 atm, and methane/oxygen/helium flames up to 60 atm. These pressure levels are substantially higher than those associated with the laminar burning velocities in the literature. As such, the data are useful in their own right for engine simulations (up to 20 atm) and for the compilation and validation of methane kinetics up to 60 atm. Our own simulations using the well-developed GRI-MECH 3.0 show substantial deviations for pressures above the range of 20–40 atm. Further work is needed to identify the causes of these deviations and avenues for remedy.

Experimental observations also showed that the outwardly propagating methane/air flames are either not wrinkled at the lower pressures or moderately wrinkled at higher pressures. This is in sharp contrast to hydrogen/air flames that showed profuse wrinkling even at pressures of a few atmospheres. The lack of strong wrinkling, ostensibly due to the larger flame thickness, implies the relative difficulty of expanding methane/air flames to attain the state of self-acceleration [22] and hence transition to either turbulent flames or detonation waves.

Through the extraction of the global activation energies and overall reaction orders, we have also demonstrated that hydrogen/air and methane/air flames exhibit the same second and third explosion limit behavior commonly associated with homogeneous hydrogen/oxygen mixtures. In particular, with increasing pressure and for suitable mixtures, the global activation energy can increase and then decrease, while the overall reaction order can decrease and then increase. It is particularly noteworthy that the changeover in behavior for methane/air flames occurs at the relatively low pressures of a few atmospheres. The need to consider intricate chemistry in the simulation of practical phenomena cannot be overemphasized.

Acknowledgments

It is a pleasure to acknowledge the generous help of Professor Frederick L. Dryer and Ms. Yolanda Stein with the GC analysis. This work was supported by the US Air Force Office of Scientific Research and NASA.

REFERENCES

1. Smith, G. P., Golden, D. M., Frenklach, M., Moriarty, N. W., Eiteneer, B., Goldenberg, M., Bowman, C. T., Hanson, R. K., Song, S., Gardiner Jr., W. C., Lissianski, V., and Qin, Z., GRI-Mech homepage, Gas Research Institute, Chicago, 1999, www.me.berkeley.edu/gri_mech/.
2. Frenklach, M., Wang, H., and Rabinowitz, M. J., *Prog. Energy Combust. Sci.* 18:47–73 (1992).
3. Law, C. K., Sung, C. J., and Wang, H., *On the Development of Detailed and Reduced Reaction Mechanisms for Combustion Modeling,* AIAA paper 2000-0806.
4. Bowman, C. T., personal communication, 2001.
5. Hassan, M. I., Aung, K. T., and Faeth, G. M., *Combust. Flame* 115:539–550 (1998).
6. Gu, X. J., Haq., M. Z., Lawes, M., and Woolley, R., *Combust. Flame* 121:41–58 (2000).
7. Wu, C. K., and Law, C. K., *Proc. Combust. Inst.* 20:1941–1949 (1985).
8. Vagelopoulos, C. M., Egolfopoulos, F. N., and Law, C. K., *Proc. Combust. Inst.* 25:1341–1347 (1994).
9. Vagelopoulos, C. M., and Egolfopoulos, F. N., *Proc. Combust. Inst.* 27:513–519 (1998).
10. Van Maaren, A., Thung, D. S., and De Goey, L. P. H., *Combust. Sci. Technol.* 96:327–344 (1994).
11. Eberius, H., and Kick, Th., *Ber. Bunsen-Ges. Phys. Chem.* 96:1416–1419 (1992).
12. Tse, S. D., Zhu, D. L., and Law, C. K., *Proc. Combust. Inst.* 28:1793–1799 (2000).
13. Rozenchan, G., "An Experimental Study of Outwardly-Propagating Hydrogen and Methane Flames at High

Pressures," M.S.E. thesis, Princeton University, Princeton, NJ, 2001.
14. Dowdy, D. R., Smith, D. B., Taylor, S. C., and Williams, A., *Proc. Combust. Inst.* 23:325–332 (1990).
15. Taylor, S. C., "Burning Velocity and the Influence of Flame Stretch," Ph.D. thesis, University of Leeds, 1991.
16. Brown, M. J., McLean, I. C., Smith, D. B., and Taylor, S. C., *Proc. Combust. Inst.* 26:875–881 (1996).
17. Kee, R. J., Grcar, J. F., Smooke, M. D., and Miller, J. A., Sandia report SAND85-8240.
18. Frenklach, M., Wang, H., Goldenberg, M., Smith, G. P., Golden, D. M., Bowman, C. T., Hanson, R. K., Gardiner, W. C., and Lissianski, V., *GRI-Mech: An Optimized Detailed Chemical Reaction Mechanism for Methane Combustion,* Gas Research Institute topical report GRI-95/0058, Gas Research Institute, Chicago, 1995.
19. Bowman, C. T., Hanson, R. K., Davidson, D. F., Gardiner Jr., W. C., Lissianski, V., Smith, G. P., Golden, D. M., Frenklach, M., and Goldenberg, M., GRI-Mech homepage, Gas Research Institute, Chicago, 1994, www.me.berkeley.edu/gri_mech/.
20. Bradley, D., and Harper, C. M., *Combust. Flame* 99:562–572 (1994).
21. Gostintsev, Yu. A., Istratov, A. G., and Shulenin, Yu. V., *Combust. Explos. Shock Waves* 24:63–70 (1988).
22. Filyand, L., Sivashinsky, G. I., and Frankel, M. L., *Physica D* 72:110–118 (1994).
23. Bechtold, J. K., and Matalon, M., *Combust. Flame* 67:77–90 (1987).
24. Landau, L. D., *Acta Physicochim. U.R.S.S.* 19:77–85 (1944).
25. Clavin, P., *Prog. Energy Combust. Sci.* 11:1–59 (1985).
26. Egolfopoulos, F. N., Zhu, D. L., and Law, C. K., *Proc. Combust. Inst.* 23:471–478 (1990).
27. Sun, C. J., Sung, C. J., He, L., and Law, C. K., *Combust. Flame* 118:108–128 (1999).
28. Law, C. K., and Sung, C. J., *Prog. Energy Combust. Sci.* 26:459–505 (2000).
29. Egolfopoulos, F. N., and Law, C. K., *Combust. Flame* 80:7–16 (1990).
30. Glassman, I., *Combustion, 3rd ed.,* Academic Press, San Diego, 1996.
31. Dougherty, E. P., and Rabitz, H., *J. Chem. Phys.* 72:6571–6586 (1980).
32. Westbrook, C. K., and Dryer, F. L., *Prog. Energy Combust. Sci.* 10:1–57 (1984).

COMMENTS

Ralph Aldredge, University of California, Davis, USA. How large was the confinement of the outwardly propagating flames? Was the growth rate of the Darriens-Landau instability estimated? Could it be that the flames were hydrodynamically unstable but that the instability was not expressed because there wasn't enough time (the confinement wasn't large enough?)

Author's Reply. The diameter of the inner chamber was 82.5 mm. We did not estimate the growth rate of the Darrieus-Landau instability, but we did observe instabilities for flames that were smooth up to a certain diameter (our maximum radius for measurements was 20 mm) and cracked beyond that limit. It is reasonable to expect that all flames will eventually become unstable when they have grown to a sufficiently large size so that stretch effects are minimized and the instabilities have enough time to grow.

•

V. Karlin, University of Central Lancashire, UK. Can you estimate the amplitude of velocity fluctuations in the mixture before ignition?

Author's Reply. We waited from 10 to 30 min for the velocity fluctuations from turbulent mixing to die down. Mixture homogeneity was verified by the Schlieren images.

•

Jan P. Hessler, Argonne National Laboratory, USA. I would like to comment on the issue of simply replacing the efficiency for collisional deactivation by helium by the efficiency for argon. Several years ago, Assa Lifshitz provided a prescription for estimating the change in efficiencies for different colliders. These scale as the square root of the ratio of the reduced masses. Albert F. Wagner has discussed this in his plenary lecture [1]. I would like to suggest that these ideas might easily be incorporated into your reaction mechanism.

REFERENCE

1. Wagner, Albert F., *Proc. Combust. Inst.* 29:1173 (2002).

Author's Reply. We carried out a comprehensive literature search on the third-body efficiency of helium but could not incorporate the information into our model since the results in the literature are for measured reactions, while the GRI is a mathematically optimized reaction mechanism. Therefore, the individual elementary reactions cannot be replaced or modified separately because they have no physical meaning outside of the mechanism. We appreciate your suggestion and will incorporate this efficiency estimation in the reaction mechanism in our future simulations.

•

Hong G. Im, University of Michigan, USA. Have you tried to normalize the Markstein length by the flame thickness to obtain the Markstein number? If the normalized Markstein number is insensitive to stretch, then this result may suggest that the real flame thickness (instead of the nominal thickness based on diffusivity and flame speed) is a more appropriate quantity to define the Markstein number.

Author's Reply. For weakly stretched flames, the Markstein length is a constant in itself and hence is insensitive to stretch. Since the actual flame thickness and the nominal flame thickness (as defined in the comment) are both constants, normalization using either of them would yield a constant.